POLITECNICO DI TORINO
Repository ISTITUZIONALE

Development of a Thermal-Hydraulic Model for the European DEMO TF Coil

(Article begins on next page)

17 July 2024

Development of a Thermal-Hydraulic Model for the European DEMO TF Coil

Roberto Zanino, *SeniorMember, IEEE*, Roberto Bonifetto, Ortensia Dicuonzo, Luigi Muzzi, *SeniorMember, IEEE*, Giuseppe F. Nallo, Laura Savoldi, *Member, IEEE*, Simonetta Turtù, *SeniorMember, IEEE*

Abstract— **In the framework of the "roadmap to fusion electricity by 2050", the design of the European DEMO machine strongly relies on available technologies. The superconducting Toroidal Field (TF) magnets will be built using available Low-Temperature Superconducting (LTS) strands; the ENEA Winding Pack (WP) proposal will exploit graded layer-wound rectangular conductors, whose design is ongoing. The WP will be encapsulated in a stainless steel casing, whose cooling has not been designed yet. In this paper, we present the thermal-hydraulic (TH) model of an entire TF coil for the European demonstration power plant DEMO. Two cooling options are proposed and investigated for the casing, while for the WP the ENEA design, with multiple low-impedance hydraulic channels, is considered. The thermal coupling between WP and casing is parametrically included in the model. The TH behavior of a TF coil (WP + casing) during a plasma burn is presented and discussed, comparing the two cooling options of the casing.**

Index Terms—**DEMO, modeling, TF coil, thermal-hydraulics.**

I. INTRODUCTION

While ITER is being built in Cadarache, France, a European "roadmap to fusion electricity by 2050" has been recently approved by the European Commission [1]. It foresees the design of a European DEMO reactor as the step following ITER, aimed at the production of electricity from fusion energy.

The DEMO superconducting (SC) magnets [2] will pose some new challenges compared to ITER, related to the increased size [3]. The DEMO toroidal field (TF) magnets, composed by a winding pack (WP) without radial plates (as opposed to ITER TF coils) and encapsulated in a steel casing, should be designed to guarantee a temperature margin $\Delta T_{mar} \equiv T_{CS} - T_{op}$ (where T_{CS} is the current sharing temperature, i.e. the temperature at which the transport current in the cable equals its critical

current, and T_{op} the operating temperature) larger than the minimum value of 1.5 K prescribed in the DEMO design criteria [4], where T_{op} is assumed equal to the inlet temperature of the Supercritical Helium (SHe) + at least 0.1 K.

Here we present the thermal-hydraulic (TH) model of an entire TF coil for the EU DEMO, developed using the 4C code [5], which was validated and applied in recent years to the SC magnet systems of several tokamaks, either operating (EAST [6], KSTAR [7]) or under construction (ITER [8-10], JT-60SA [11]).

A design of the TF casing cooling, considering two options, is proposed here for the first time, and a detailed model for the casing and WP cooling is developed. The most recent (2014) WP design for the double-layer wound DEMO TF coils, proposed by ENEA [12-13], is considered here, with rectangular cable-in-conduit conductors (CICC) cooled by SHe and layer-wound to obtain a graded (Nb_3Sn + NbTi) WP. Differently from [12-13], the SHe flows in the CICC in two low-impedance channels, see Fig. 1, instead of the customary single one [14-16], to follow the latest ENEA development in the conductor design for the European DEMO.

The new DEMO TF model is intrinsically transient, but is applied here to the TH analysis of the steady-state plasma burn scenario, when a non-negligible nuclear heat load is deposited on the magnet. The resulting minimum ΔT_{mar} over the entire

R. Bonifetto, O. Dicuonzo, G.F. Nallo, L. Savoldi and R. Zanino are with NEMO group, Dipartimento Energia, Politecnico di Torino, Torino, 10129 Italy (e-mail: laura.savoldi@polito.it).
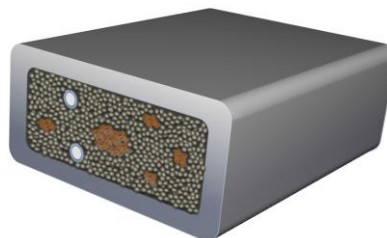L. Muzzi and S. Turtù are with ENEA, Frascati, Italy.

Fig. 1. ENEA design of the conductor for the innermost layer of the European DEMO TF WP. The white circles represent the two low-impedance channels. The apparent non-uniformity of the cooling provided by the asymmetry of the channels on the cross section is due to their twist with the respective petals: the uniformity is guaranteed *on average* along the whole length.

WP is evaluated by the 4C code, together with the temperature distribution in the casing, depending on the different casing cooling options.

II. DESIGN OF THE CASING COOLING

Preliminary simulations, not shown here, proved that in the absence of casing cooling the nuclear heat load deposited in the casing is transferred directly to the WP and could lead to a quench, depending on the thermal coupling (i.e., the heat flux transferred) between neighbouring layers of the WP across the turn and layer insulation [15], see also below.

The design of the casing cooling proposed here foresees as in ITER the use of casing cooling channels (CCCs) inserted into grooves manufactured inside the casing, see Fig. 2 and Fig. 3. The CCCs are grouped in two parallel branches, see Fig. 3: the first one includes all CCCs on the inboard leg; the other includes the CCCs on the outboard leg.

Two different options (and the corresponding models) for the routing of the casing cooling circuit have been developed. As a common feature, both cooling options provide fresh SHe to the plasma-side channels, which are the most critical ones, and assume in these the same mass flow rate/channel.
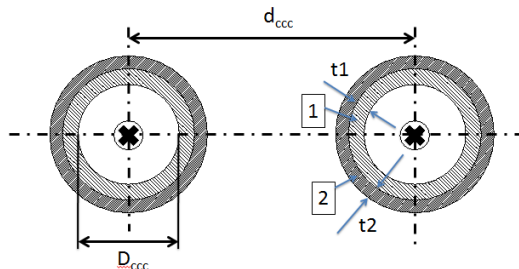

Fig. 2. Geometry and structure of a CCC. 1 = jacket, 2 = insulation. $t1 = 1.245$ mm, $t2 = 1$ mm, $D_{ccc} = 7.8$ mm, $d_{ccc} = 54$ mm for the front channels, $d_{ccc} = 108$ mm for the remaining channels.
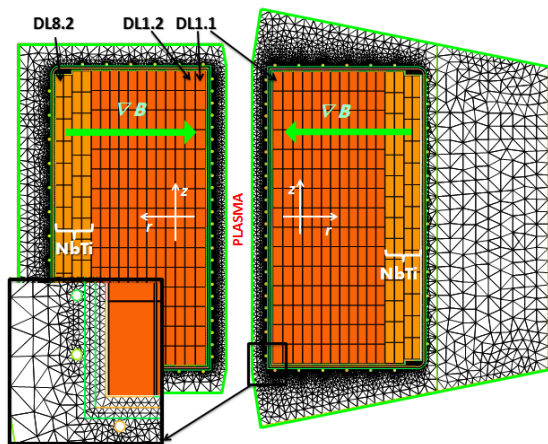

Fig. 3. Schematic view of the cross section of an EU DEMO TF coil, including WP and casing. Left: outboard leg cross section, Right: inboard leg cross section. The inset shows a zoom highlighting the CCCs.
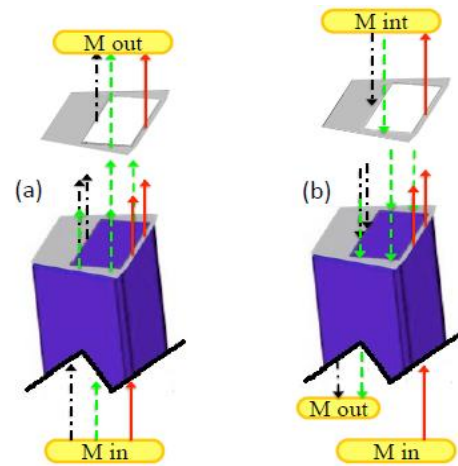

Fig. 4. Schematic view of the two configurations analyzed for the casing cooling circuit: front (plasma-side) channels: solid red lines; side channels: dashed green lines; back channels: dash-dotted black lines. The inlet and outlet manifolds are labelled "M in" and "M out", respectively; "M int" is the intermediate manifold.

As to the differences we have:

a) A "once through" configuration, where the SHe flows in all CCCs from the bottom to the top of the coil, then enters a manifold in order to be recirculated through the helium bath, see Fig. 4a. The total mass flow rate in the CCCs is chosen for this design equal to that of ITER (0.15 kg/s [17]). This design, which is the most conservative from the cooling point of view, requires however the largest mass flow rate from the cold circulator.

b) A "total rerouting" configuration, where the He from the plasma-side channels is re-routed to and distributed among the remaining channels, see Fig. 4b. This design will require the minimum mass flow rate but will be at the same time the least conservative from the cooling point of view.

III. CASING MODEL

We model here the TF casing corresponding to the 2014 WP design, using the 4C code [5]. A coarse poloidal discretization is used; depending on the poloidal location, two different cross sections have been accounted for, see Fig 3, representative of the outboard and inboard legs, respectively.

A. Model of the structure

The geometrical parameters used as inputs for the 2D heat conduction model are taken from [18]. The glass epoxy ground insulation (GI) surrounding the WP is considered, as well as an insertion gap (filled with epoxy resin) between the former and the casing, see inset in Fig. 3. The thermal conductivity k_{GI} of the GI has been varied parametrically from zero
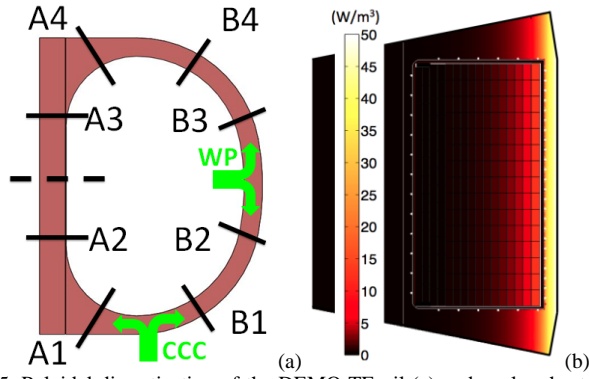
Fig. 5. Poloidal discretization of the DEMO TFcoil (a) and nuclear heat load distribution on an inboard poloidal cross section (b). In (a) the dashed line represents the equatorial plane, and the inlets of the casing cooling circuit and of the winding cooling circuit are highlighted.

(fully insulated) to its nominal value (perfect contact), to account for the effect of a possible gap opening during operation. The same recipe was already adopted for ITER TF coils [9], where the nominal k_{GI} value was consistent with [19]. The grid used for the present analysis (checked for grid independent results), is shown in Fig. 3. In the poloidal direction, 8 cuts have been checked to be enough for the discretization of the solid domain (see Fig. 5a), for the transient considered here.

B. Model of the casing cooling channels

The standard set of 1D conservation laws is solved to compute the transient evolution of the SHe velocity v, pressure p and temperature T along each channel [20]. The thermal coupling between the CCC and the casing is modeled as an equivalent thermal resistance accounting for 1 mm of glue (epoxy).

The total SHe mass flow rates in the CCCs for the configurations a) and b) of Fig. 4 are assumed to be ~0.15 kg/s and ~0.075 kg/s, respectively.

IV. CONDUCTOR AND WP MODEL

According to the new ENEA design, the conductor of double-layer (DL) 1 is obtained from a six-petal circular conductor squeezed to a rectangular shape, where two petals are wound around two small spirals, see Fig. 1. After this process, the two spirals result into two low-impedance cooling channels ("holes") - this solution should avoid the collapse of a central channel during the compaction of the rectangular CICC with high aspect ratio and low void fraction. The concept of a "distributed" pressure relief channel, already proposed for the Korean DEMO magnet system [21], is developed considering that: a) at least the same cross-section for

the coolant inside the open channels, as for the initial design, needed to be maintained; b) the number of open channels should be > 1, so that in case one channel could be subject to a severe deformation in some conductor position, another un-deformed channel could be available to recover the flow locally blocked, through a transverse fluid flow exchange. For the same reason, in the final choice the two channels were not placed in symmetrical petals.

The main parameters of the new conductor are reported in Table I.

A. Model of the new ENEA conductor

The classical approach of [20] is adopted: transient 1D heat conduction equations describe the evolution of the temperature along the jacket and the strands, respectively, while three sets of 1D conservation laws account for the transient evolution of the SHe v, p and T profiles along the bundle region (B) and the two holes ($H1$, $H2$), respectively.

Standard friction factor correlations are adopted, i.e. the Darcy-Forcheimer correlation for the flow in porous media [22] in B, and a correlation for helically ribbed channels [23] in $H1$ and $H2$. The convective heat transfer coefficient is computed according to the Dittus-Boelter correlation [24] in B, $H1$ and $H2$, as already done in the past (see [15] and [20] and refs therein). The mass, momentum and heat transfer between B and $H1$/$H2$ is allowed through the perforated surface of the respective spirals, and it is driven by the local pressure difference [20]. The heat transfer through the thickness of the helices is also described by a simple thermal-resistance model.

TABLE I
MAIN PARAMETERS FOR THE DL1 (AND DL2) CONDUCTORS

|		
Conductor	Hydraulic length [m]	548.1 (557.0)
	Total Helium cross section [mm^2]	447.0 (395.5)
	Wetted perimeter conductor-helium [m]	4.1 (4.5)
	Void fraction	0.26(0.2513)
Cooling channel #1	Inner diameter [mm]	5 (6)
	Outer diameter [mm]	7 (10)
	Fraction of spiral void	0.4 (0.4)
Cooling channel #2	Inner diameter [mm]	5 (-)
	Outer diameter [mm]	7 (-)
	Fraction of spiral void	0.4 (-)
Jacket	Inner size [mm^2]	24.78 × 66.58 (22.5 × 69.4)
	Thickness [mm]	7.01 (8.07)
Turn insulation	Outer size [mm^2]	45.2 × 88.8 (41.9 × 88.8)
Cosθ		0.95 (0.95)
SC strands	Number	1080 (480)
	Diameter [mm]	1 (1)
	Cu/nonCu ratio	1 (1)
Cu segregated strands	Number	132 (816)
	Diameter [mm]	1.5 (1)
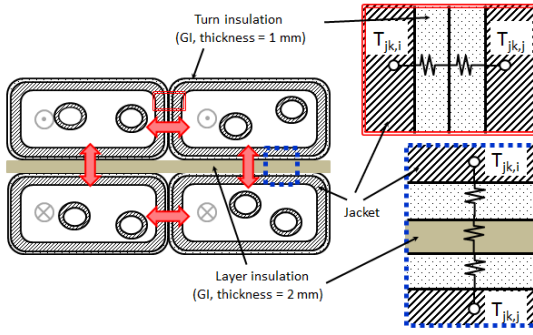
Fig. 6. Schematic view of the model for the thermal coupling between conductors in the WP.

B. Model of the European DEMO TF WP

The WP is composed by 8 conductors wound in double layers (DLs). Each layer is independently cooled, so that the WP is cooled by 16 parallel paths, see Fig. 3. Both the inlets and the outlets are located on the outboard equatorial plane, see Fig. 5a. Each conductor is in direct thermal contact with the neighboring one(s) through a series of inter-turn and inter-layer thermal resistances, see Fig. 6 [25].

V. MODEL OF THE COOLING CIRCUITS

To provide consistent boundary conditions to the conductors and CCCs, a rough model for the cooling circuit has been introduced here both for the WP and the casing. The circuits are similar to those previously developed for the ITER TF analyses [8-10], see Fig. 7. The main parameters of the components included in the model, needed to obtain a first estimation of total He volume in the circuits and transit time-scales, are specified in Table II.

VI. ANALYSIS OF A PLASMA BURN SCENARIO

A. Input

The scenario analyzed here is the standard plasma burn [26]. We consider the TF operating @ $I = 81.7$ kA, with the magnetic self-field distribution described in [15] and assuming a uniform mechanical strain of –0.55 % acting on the Nb_3Sn. The superconductor critical properties are the same adopted in [15]. The (uniform) nuclear heat load, as estimated in [27] (see Fig. 5b), is applied on each layer, while an exponential decay starting from the plasma side is applied to the casing. The overall heat deposited is 182.2 W in the WP and 218.8 W in the casing. Starting from an initial temperature of 4.5 K in both casing and WP, a mass flow rate of ~6 g/s in each Nb_3Sn layer, ~8 g/s in each NbTi layer and

TABLE II
MAIN PARAMETERS OF THE DEMO TF COOLING CIRCUITS

Component	Name	Characteristics	
		Length (m)	Diameter (mm)
Pipes	$Feeder_{in}^W$	20	44
	$Feeder_{out}^W$	20	44
	$Cryoline_{W1}$	140	44
	$Cryoline_{W2}$	140	44
	$Feeder_{in}^C$	20	39
	$Feeder_{out}^C$	25	39
	$Cryoline_{C1}$	30	39
	$Cryoline_{C2}$	30	39
		Bath temperature (K)	Heat transfer area (m^2)
Heat Exchangers	HX_W	4.5	37
	HX_C	4.5	37
		Nominal pressure drop (Pa)	
Valves	CV_{W1}	1000	
	CV_{W2}	1000	
	CV_{C1}	10000	
	CV_{C2}	5000	
		Type	
Pumps	$Pump_W$	Centrifugal pump	
	$Pump_C$	Centrifugal pump	

~1.5 g/s in each CCC (in the "once through" configuration) is circulated, with an inlet pressure of 0.6 MPa (and a corresponding pressure drop of ~1 bar on the entire WP); the full transient is followed up to the establishment of a steady state, which is then analyzed. In view of the assumed almost perfect nature of the HX_W in Fig. 7, the temperature of the SHe at the inlet of the WP is very close to that of the bath, i.e., 4.5 K, see Table II.

B. Results

Despite the fact that the magnetic field in DL2 is lower than in DL1, the lowest T_{CS} (~5.97 K) is computed (with reference to [28]) in DL2.1, because of the lower superconductor cross section (see Table I). On the other hand, the operating temperature computed by 4C is obviously higher, the closer the layer is to the plasma, but even artificially assuming negligible inter-layer heat transfer, see Fig. 6, DL2.1 does not become cold enough to compensate the lower T_{CS}, so that the minimum temperature margin (~0.7 K) is computed by 4C in DL2.1, see Fig. 8.
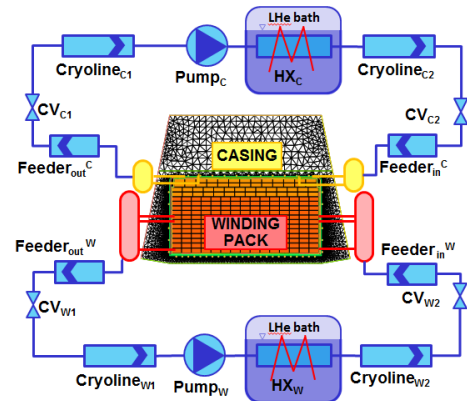

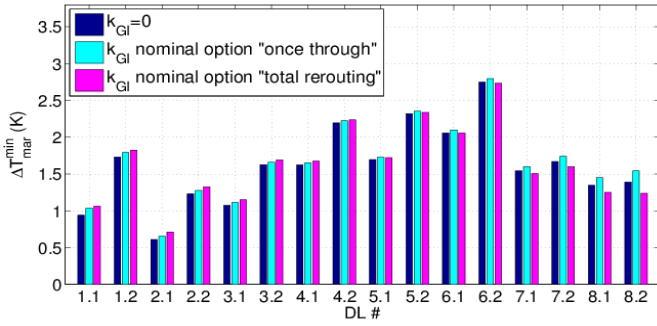Fig. 7. Schematic of the model of the WP and casing cooling circuits.

Fig. 8. Computed minimum ΔT_{mar} in each layer. Effect of k_{GI} and comparison between casing cooling option "once-through" and "total rerouting".

Therefore, while according to the definition in [4] the design criteria are marginally satisfied ($\Delta T_{mar} = 5.97 - (4.5 + 0.1) \sim 1.4$ K), the nuclear heating effectively erodes a significant fraction of this margin in DL2.1, but also in other layers.

The thermal coupling to the casing, $k_{GI} \neq 0$ in Fig. 8 in option a) ("once-through"), provides additional cooling to the WP, slightly increasing the margin. Indeed, the casing cooling is so effective that the power removed by the casing coolant (~231 W) is even larger than the power deposited by nuclear heating in the casing (~219 W). The situation is reversed if option b) ("total rerouting") is adopted, since only 170 W are removed by the casing coolant, leading globally to an additional load on the WP. However, this effect should be considered locally rather than globally: the additional load on the casing is concentrated on the outermost layers, and results in a temperature margin reduction in the outer DLs (see Fig. 8), while the heat removal is very efficient on the inner DLs, leading to an increase in their margin. The magnitude of the cooling effect of the CCCs on the WP is influenced by the thermal coupling between CCCs and casing, which should be investigated parametrically [29].

The computed temperature map in a selection of the casing cuts, see Fig. 5a, is reported in Fig. 9,
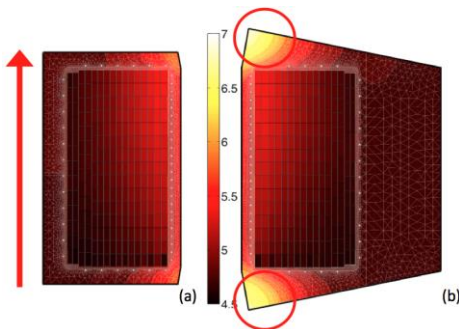

Fig. 9. Computed temperature map in the cuts B3 (a) and A3 (b), respectively, in the "once through" configuration, for the nominal k_{GI}. The red arrow on the left shows the direction of the cooling He.

showing that the peak temperature is reached in the corners of the wedged region of the inboard leg (Fig. 9b), where no CCCs are currently foreseen. Indeed, a revision of the design could be considered, actively cooling those regions, to reduce the temperature gradients which could arise during, e.g., the cool-down. In the outboard section, some (top/bottom) asymmetry induced by the fact that the fresh He is entering from the bottom in Fig. 9a is also visible.

C. Impact of the different CCC configurations

Option b) for the casing cooling leads to a casing temperature increase ΔT up to 0.5 K with respect to the "once-though" configuration, option a), in view of the higher He inlet temperature in the side and back channels. This ΔT corresponds to a leveling of internal energy inside the casing and is negligible in absolute terms. The two different cooling options should be compared also with reference to other operating conditions, such as the magnet cool-down.

VII. CONCLUSIONS AND PERSPECTIVE

A first design of the EU DEMO TF casing cooling, through channels inserted into grooves, has been presented considering two routing options. The thermal-hydraulic model of a TF coil for the EU DEMO, including the coil casing and the cooling circuits for both WP and casing, has also been developed with the 4C code, based on the 2014 ENEA design for the WP.

The thermal-hydraulics of a standard plasma scenario (steady-state burn) has been studied, showing that the ΔT_{mar} is significantly eroded by nuclear heating. The casing cooling option b), which foresees the total rerouting of the plasma-side CCCs, appears preferable, as it needs only half of the total mass flow rate in the CCCs compared to option a), but the consequent reduction of the ΔT_{mar} on the outermost (NbTi) DLs deserves some attention.

In perspective, we plan to apply the model to the new WP design proposals and to other cooling options for the casing, investigating the thermal-hydraulic behavior of the coil not only during plasma scenarios, but also during cool-down and off-normal conditions, such as quench propagation.

ACKNOWLEDGMENT

REFERENCES

[1] F. Romanelli *et al.*, "Fusion electricity. A roadmap to the realisation of fusion energy" [Online]. Available: https://www.euro-fusion.org/wpcms/wp-content/uploads/2013/01/JG12.356-web.pdf, Accessed on 18 Aug. 2015.

[2] L. Zani *et al.*, "Overview of progress on the EU DEMO magnet system design," presented at the MT-24 conference, *IEEE Trans. Appl. Supercond.*, submitted for publication, 2015.

[3] P. Bruzzone, "Pre-conceptual studies and R&D for DEMO superconducting magnets," *Fus. Eng. Des.*, vol. 89, 2014, pp. 1775–1778.

[4] L. Zani, D. Ciazynski, A. Nijhuis, and A. Torre, "Setting common operating values, analysis tools, and criteria for DEMO TF WP design," EFDA_D_2LNLLB, 07/07/2014.

[5] L. Savoldi Richard, F. Casella, B. Fiori, and R. Zanino, "The 4C Code for the Cryogenic Circuit Conductor and Coil modeling in ITER," *Cryogenics*, vol. 50, 2010, pp. 167–176.

[6] R. Zanino, R. Bonifetto, U. Bottero, J. Li, J. Qian, L. Hu, X. Gao, L. Savoldi Richard, and Y. Wu, "Application of the 4C Code to the Thermal-hydraulic Analysis of the CS Superconducting Magnets in EAST," *Cryogenics*, vol. 63, 2014, pp. 255–262.

[7] L. Savoldi Richard, R. Bonifetto, Y. Chu, A. Kholia, S. H. Park, H. J. Lee, and R. Zanino, "4C code Analysis of Thermal–hydraulic Transients in the KSTAR PF1 Superconducting Coil," *Cryogenics*, vol. 53, 2013, pp. 37–44.

[8] L. Savoldi Richard, R. Bonifetto, A. Foussat, N. Mitchell, K. Seo, and R. Zanino, "Mitigation of the Temperature Margin Reduction due to the Nuclear Radiation on the ITER TF Coils," *IEEE Trans. Appl. Supercond.*, vol. 23, no. 3, Jun. 2013, Art. ID 4201305.

[9] L. Savoldi Richard, R. Bonifetto, U. Bottero, A. Foussat, N. Mitchell, K. Seo, and R. Zanino, "Analysis of the effects of the nuclear heat load on the ITER TF magnets temperature margin," *IEEE Trans. Appl. Supercond.*, vol. 24, no. 3, Jun. 2014, Art. ID 4200104.

[10] L. Savoldi Richard, D. Bessette, R. Bonifetto, and R. Zanino, "Parametric Analysis of the ITER TF Fast Discharge using the 4C code," *IEEE Trans. Appl. Supercond.*, vol. 22, 2012, Art. ID 4704104.

[11] R. Bonifetto, P. K. Domalapally, G. M. Polli, L. Savoldi Richard, S. Turtù, R. Villari, and R. Zanino, "Computation of JT-60SA TF coil temperature margin using the 4C code," *Fus. Eng. Des.*, vol. 86, 2011, pp. 1493–1496.

[12] P. Bruzzone, K. Sedlak, D. Uglietti, N. Bykovsky, L. Muzzi, G. De Marzi, G. Celentano, A. della Corte, S. Turtù, and M. Seri, "LTS and HTS high current conductor development for DEMO," *Fus. Eng. Des.*, vol. 96-97, 2015, pp. 77–82.

[13] P. Bruzzone, K. Sedlak, B. Stepanov, L. Muzzi, S. Turtù, A. Anemona, and J. Harman, "Design of Large Size, Force Flow Superconductors for DEMO TF Coils," *IEEE Trans. Appl. Supercond.*, vol. 24, no. 3, Jun. 2014, Art. ID 4201504.

[14] L. Savoldi, R. Bonifetto, L. Muzzi, and R. Zanino, "Quench Propagation in the European DEMO TF Coil Winding Pack: a First Analysis with the 4C Code," *IEEE Trans. Plasma Science*, submitted for publication, 2015.

[15] L. Savoldi, R. Bonifetto, L. Muzzi, and R. Zanino, "4C Code Analysis of High-Margin Quench Propagation in a DEMO TF Coil," Proceedings of the 26th Symposium on Fusion Engineering (SOFE26), Austin, Texas, May 31 – June 4, 2015.

[16] R. Vallcorba *et al.*, "Thermo-hydraulic analyses associated to a design proposal for DEMO TF conductor," presented at CHATS on Applied Superconductivity, Bologna, Italy, September 14-16, 2015.

[17] ITER Design Description Document: DDD 11-2. TF Coils and Structures, ITER_D_2MVZNX, v2.2, 2009.

[18] K. Sedlak, and P. Bruzzone, "WP#1 Initial Design," EFDA_D_2LKMES, v. 1.0, 18/11/2014.

[19] ITER Design Requirements and Guidelines Level 1: DRG 1 Structural Material Database Article 3. Non-Metallic Materials Database & Specifications—Electrical Insulation Materials, ITER_D_223AXS, v1.0.

[20] R. Zanino, S. De Palo, and L. Bottura, "A two-fluid code for the thermohydraulic transient analysis of CICC superconducting magnets," *J. Fus. Energy*, 1995, pp. 14–25.

[21] K. Kim, S. Oh, J. S. Park, C. Lee, K. Im, H. C. Kim, G.-S. Lee, G. Neilson, T. Brown, C. Kessel, P. Titus, and Y. Zhai, "Conceptual design study of the K-DEMO magnet system," *Fus. Eng. Des.*, vol. 96–97, Oct. 2015, pp. 281–285.

[22] M. Bagnasco, L. Bottura, and M. Lewandowska, "Friction factor correlation for CICC's based on a porous media analogy," *Cryogenics*, vol. 50, 2010, pp. 711–719.

[23] R. Zanino, S. Giors, and L. Savoldi Richard, "CFD modeling of ITER cable-in-conduit superconductors. Part III: correlation for the central channel friction factor," Proceedings of the 21st International Cryogenic Engineering Conference (ICEC21), Prague, July 17 – 21, 2006, vol. 1, 2007, pp. 207–211.

[24] F. P. Incropera, and D. Dewitt, "Fundamentals of Heat and Mass Transfer," 6th ed., New York, NY, USA: Wiley & Sons, 2006.

[25] L. Savoldi and R. Zanino, "M&M: Multi-conductor Mithrandir code for the simulation of thermal-hydraulic transients in superconducting magnets," *Cryogenics*, vol. 40, 2000, pp. 179–189.

[26] R. Kemp, "DEMO design summary," EFDA_D_2L2F7V, v1.0, 24/05/2012.

[27] L. Zani, and U. Fischer, "Advanced definition of neutronic heat load density map on DEMO TF coils," EFDA_D_2MFVCA, 18/10/2014.

[28] L. Bottura, and B. Bordini, "Jc(B, T, ε) Parameterization for the ITER Nb3Sn production," *IEEE Trans. Appl. Supercond.*, vol. 19, no. 3, Jun. 2009, pp. 1521–1524.

[29] C. Hoa, B. Rousset, B. Lacroix, S. Nicollet, R. Vallcorba, D. Bessette, A. Vostner, and F. Gauthier, "Experimental characterization of the ITER TF structure cooling in HELIOS test facility," presented at the CEC conference, Tucson, AZ, USA, June 28 – July 2, 2015.